Systematic Evaluation of Food design, Treatments, Packaging and Storage Conditions on Microplastic Concentrations in Complex Matrices

Guyu Peng , Orasai Faikhaw , Bibiana Juan , Thorsten Reemtsma

PII: S2772-4166(25)00383-3
DOI: https://doi.org/10.1016/j.hazadv.2025.100972
Reference: HAZADV 100972

To appear in: *Journal of Hazardous Materials Advances*

Received date: 28 September 2025
Revised date: 7 December 2025
Accepted date: 11 December 2025

Please cite this article as: Guyu Peng , Orasai Faikhaw , Bibiana Juan , Thorsten Reemtsma , Systematic Evaluation of Food design, Treatments, Packaging and Storage Conditions on Microplastic Concentrations in Complex Matrices, *Journal of Hazardous Materials Advances* (2025), doi: https://doi.org/10.1016/j.hazadv.2025.100972

Highlights

- Systematic evaluation of microplastics in multiple food samples pre-consumption.
- Matrix-specific digestion protocols developed for milk, plant milk and juice.
- Acidic food and plastic packaging contributed more to microplastics levels.
- Thermal treatment or storage time showed no significant effects.
- FTIR imaging with chemometrics overcame matrix interferences.

Systematic Evaluation of Food design, Treatments, Packaging and Storage Conditions on Microplastic Concentrations in Complex Matrices

Guyu Peng[1*], Orasai Faikhaw[1], Bibiana Juan [2,*], Thorsten Reemtsma [1,3,*]

[1] Helmholtz Centre for Environmental Research - UFZ, Department of Environmental Analytical Chemistry, Leipzig, 04318, Germany

[2] Centre d'Innovació, Recerca i Transferència en Tecnologia dels Aliments (CIRTTA), TECNIO (CERTA-UAB), Departament de Ciència Animal i dels Aliments, Facultat de Veterinària, Universitat Autònoma de Barcelona (Cerdanyola del Vallès), 08193 Barcelona, Spain

[3] University of Leipzig, Institute for Analytical Chemistry, Linnestrasse 3, 04103, Leipzig, Germany

*Correspondence: G. Peng: guyu_peng@hotmail.com, B. Juan: Bibiana.juan@uab.cat, T. Reemtsma: thorsten.reemtsma@ufz.de

Abstract

Worldwide, 44% of plastic products are used as packaging materials, exposing humans to micro(nano)plastics potentially through food ingestion. Here, we evaluated the microplastic concentrations throughout the pre-consumption phase, considering the effects of food design (milk, plant milk and orange juice), treatment (thermal), packaging (glass and polypropylene) and storage duration (0, 90 and 180 days). Due to the rich organic matter in food samples, more than 12 digestion protocols were tested and optimized to establish matrix-specific digestion protocols. Microplastics (> 10 μm) from milk, tiger nut milk and orange juice samples were quantified using micro-Fourier-transform infrared (μ-FTIR) imaging. The microplastic concentrations were 37 ± 34 n/100 mL milk, 18 ± 19 n/100 mL tiger nut milk, and 62 ± 68 n/100 mL orange juice samples, suggesting that acidic food environments released more microplastics. PP was the most frequently detected polymer, followed by polyethylene terephthalate fibers and polystyrene, indicating the contribution from plastic packaging and the ambient environment. No significant difference was observed among thermally treated and non-treated, or various storage duration groups for the three food types. A majority (69%) of detected microplastics were below 50 μm. Chemometric analyses revealed spectral interference from the matrix with the IR spectra of plastic polymers. This study provides the first systematic evaluation of the MP concentrations across multiple food types during commercial food processing, packaging and storage steps pre-consumption, that determined human exposure to microplastics via food intake to guide future mitigation strategies.

Keywords: **microplastics, food analysis, matrix digestion, FTIR imaging, food packaging, diet exposure**

Highlights

- Systematic evaluation of microplastics in multiple food samples pre-consumption.
- Matrix-specific digestion protocols developed for milk, plant milk and juice.
- Acidic food and plastic packaging contributed more to microplastic levels.
- Thermal treatment or storage time showed no significant effects.
- FTIR imaging with chemometrics overcame matrix interferences.

1. Introduction

Worldwide, 44% of plastic products are used as packaging materials (PlasticsEurope, 2022). Plastic food-contact materials (PFCM) have raised new health concerns regarding the release of micro(nano)plastics (MNPLs) (Liang et al., 2023). Food packaging is the primary source of microplastics (MPs) and nanoplastics (NPs) in food and water, leading to human exposure via food ingestion (Oliveira et al., 2019; Ter Halle and Ghiglione, 2021). Recent studies have demonstrated the migration of MNPLs from PFCMs into food (Shruti and Kutralam-Muniasamy, 2024). While most research has focused on consumer products and post-consumption preparation, data on the systematic release of MNPLs from food design, food treatment, and packaging and storage conditions prior to consumption remains scarce.

Despite growing concern regarding associated health effects (Visentin et al., 2025), major dietary items that are consumed daily, including milk, plant milk and juice are still less studied. They are nutritious and recommended for daily consumption, resulting in long-term MNPL exposure. Milk is a valuable, nutritious liquid food that provides energy, high quality protein, essential minerals and vitamins (Lock and Shingfield, 2004). Global cow milk consumption averages 10 – 212 kg per capita per year (Zhang et al., 2021). Plant-based beverages are non-diary beverages made from plants extracts, such as almond, oat, soy, and coconut milk. Plant milks have gained popularity in recent decades due to their advantages over animal milks in terms of greenhouse gas emission, water and land use, in addition to the health benefits and long consumption history in lactose-intolerence regions (Mekanna et al., 2024). Orange juice (OJ) is the most consumed fruit juice worldwide (Perez-Cacho and Rouseff, 2008).

Most commercial milk and juice products undergo heat treatment to destroy spoilage microorganism and extend shelf life. Heat treatment can extend the durability of milk from several days to several years at ambient temperatures (Rauh and Xiao, 2022). In particular, ultra-high temperature (UHT) treatment utilizes higher temperatures for just a few several seconds, effectively sterilizing the product and extending the shelf life up to eight months (Amador-Espejo et al., 2014). Similarly, commercial orange

juice products are thermally treated to reduce microbial and enzymatic activities due to its cost-effectiveness (Perez-Cacho and Rouseff, 2008). However, high temperature can also lead to thermal degradation of plastics, which may affect its physical and chemical properties and facilitates release of microplastics and its migration to food (Jadhav et al., 2021). Thermal treatment of plastic packaging increases the migration of oligomer or monomer from the container into the milk, raising potential food safety concerns (Ščetar et al., 2019).

Since the 1930s, plastic has gradually replaced glass as the primary packaging materials for milk (Alvarez and Pascall, 2011). Polypropylene (PP) is widely used in the food industry due to its good mechanical resistance, heat stability and chemical inertness, and is therefore commonly employed for packaging of beverages subjected to thermal treatments, such as milk or fruit juices. However, recent studies have highlighted that PP containers may release microplastics into food matrices, especially under conditions of elevated temperature and prolonged storage (Basaran et al., 2023; Dileepan et al., 2025; Li et al., 2020).

Although diet is the main route of microplastic (MP) exposure in humans (Vethaak and Legler, 2021), assessing external exposure through various food and beverages remain challenging. These challenges stem from the complexity of food matrices, which hinder efficient MP extraction and quantification, as well as the lack of standard analytical methods capable of detecting small-sized MP detection at low concentrations. Studies on establishing food-specific digestion protocols for MP extraction is currently scarce, and data on MPs in orange juice or plant milk with a fast growing market demand is currently absent (Ramsing et al., 2023). Therefore, this study aims to 1) develop, optimize and validate digestion and sample preparation protocols for MP analysis in cow's milk, tiger nut milk (as a type of plant milk) and orange juice, and 2) systematically investigate variation of MP concentrations in these food overtime under conditions relevant to food design, treatment, packaging and storage, to generate critical exposure data for human health risk assessment.

2. Materials and Methods

2.1 Discontinuous heat treatment of food samples and packaging and storage conditions

Cow milk was collected from morning milking and sent to UAB for treatment (Juan and Trujillo, 2022). The production of tiger nut milk was carried out as described in Codina-Torrella et al. (2023). Orange juice samples were from commercial brands purchased from Barcelona, Spain (Rizzi et al., 2024). Discontinuous heat treatments of food samples were performed using an autoclave (Model 1000-LC, Calderería Ramón Naves, S.L. Barcelona, Spain). The heat treatment processes varied depending on the food. Milk and tiger nut milk was treated at heating step (121°C, 20 minutes, 1 bar pressure), holding step (121°C, 25 minutes, 1 bar pressure) and cooling step (25°C, 20 minutes, 0 bar pressure). Orange juice was treated at heating step (100°C, 20 minutes, 1 bar pressure), holding step (100°C, 7 minutes, 0 bar pressure) and cooling step (25°C, 20 minutes, 0 bar pressure). Prior to heat treatment, all samples were packaged in 1000 mL white polypropylene (PP) bottles (Figure S1). The PP bottles were sealed with PE cap incorporating an aluminum layer between the cap and the bottle neck to prevent MP contamination from the closure. The products were then stored at room temperature (20–25 °C) and sampled at 0, 90 and 180 days. After storage, samples were frozen and maintained at -18 °C until MP analysis. A control sample (Ctrl) was included for each of the three food types, and were not subjected to any heat treatment, were packed in glass bottles and were immediately stored at -18 °C on Day 0. A schematic overview of the sample treatment processes is provided in Figure 1. A detailed list of food samples can be found in Table S1-S3.

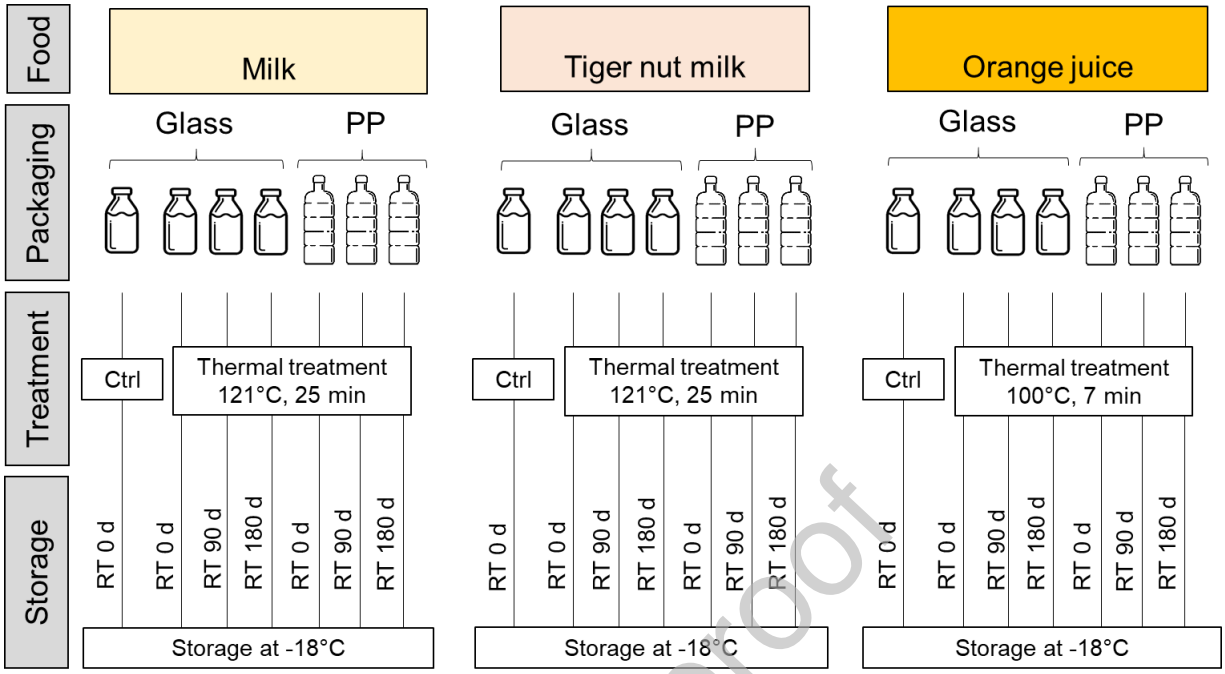

Figure 1. Schematic of packaging, discontinuous heat treatment and storage conditions of milk, tiger nut milk and orange juice samples. PP: polypropylene, RT: room temperature, Ctrl: control.

2.2 Development of digestion protocols of food samples

Raw bovine milk contains, on average, 3.5% of fat, 3.4% protein, 5% lactose, <1% salt and vitamins, 13% total solids and 87% water (Foroutan et al., 2019). Tiger nut milk (TM) "Horchata de chufa" is a beverage obtained from the aqueous extract of tiger nut tubers (*Cyperus esculentus* L.). It is one of the most consumed tiger nut-based products in Spain, characterized by its pale color and mild flavor, and comprised of more than 50% carbonhydrates, 2% fat, 1% fiber, and 1% potein (Codina-Torrella et al., 2023). Orange juice is acidic with a pH of around 3.5, and primarily composed of sugar (10%) and water (88%), and <1% fiber (Kelebek et al., 2009).

To enable reliable MP analysis in complex food matrices, optimized protocols for MP isolation via matrix digestion for milk, tiger nut milk and orange juice was developed. Standard operating procedures (SOPs) were established to ensure reproducibility and sensitivity across sample types, tailored to the requirements

of micro-Fourier-transform infrared (µ-FTIR) imaging system as implemented at UFZ (Rynek et al., 2024). For FTIR imaging in transmission mode, sample preparation utilized Anodisc filters (pore size 0.2 µm, Ø = 25 mm) as the substrate. This configuration enabled a particle size detection limit of 11 µm with a spatial resolution of 5.5 µm. Given the complex organic composition of milk, tiger nut milk and orange juice, various digestion protocols were evaluated to efficiently remove the organic background while preserving the integrity of MPs. We started from the most common digestion protocols (chemicals and enzymes) for organic matrices for MP analysis, optimized the digestion environments, and tested the maximum volume of the samples that can be digested with the protocols. The following digestion strategies and conditions were systematically tested: 1) alkaline digestion with 10% KOH; 2) alkaline digestion with 20% KOH; 3) oxidation with 30% H_2O_2; 4) oxidation with NaClO; 5) dissolution using urea/thiourea/NaOH (UTS); 6) enzymatic digestion with amylase; 7) enzymatic digestion with cellulase; 8) enzymatic digestion with cellulase and dissolution with UTS; 9) digestion in an orbital shaker/incubator; 10) digestion in a magnetic stirrer; 11) digestion at various temperatures; and 12) sample volume of 10 mL, 20, 50 and 100 mL for digestion. A combination of these protocols was also tested for digesting milk, TM and OJ. The most effective and matrix-specific protocols were selected and refined into SOPs. A detailed description of stepwise development, challenges encountered, and rationale for final protocol selection of the SOP is provided in SI Text 1. Effects of each tested protocols are provided in Figure S2-S3.

2.3 Reference materials and FTIR analysis

Identification and quantification of MPs > 10 µm on Anodisc filter were performed using an Agilent Cary 600 series FTIR spectrometer equipped with a focal plane array (FPA) detector and microscope (Agilent Technology Inc., CA, USA) operating in transmission mode. Spectra were collected over a wavenumber range of 3,800-1,250 cm^{-1} co-adding 8 scans. This spectral range was selected to avoid interference from strong absorption bands of the Anodisc filter made from aluminium oxide in the fingerprint region, which is a common practice in MP monitoring studies (Mintenig et al., 2019). During measurement, each filter

was covered with a BaF_2 window (Ø = 25 mm) to ensure a flat surface during scanning. Mosaics of the entire filter was captured with a camera, and the scanned IR spectral data were analyzed using Purency software (Purency GmbH, Vienna, Austria) that applied machine learning algorithms for automated identification of 21 types of MPs (Hufnagl et al., 2022). Although the FPA-FTIR system has a resolution of 5.5 μm per pixel, we define a "particle" as a cluster of at least 4 pixels (2 × 2) of the sample, resulting in a size detection limit of 11 μm. The similarity of the particle to the surrounding pixels (particle VS matrix) was set to 0.2, and relevance of pixels to reference spectra was set to 0.2. The performance of the particle identification software in identifying and imaging six common types of polymers were validated through spiking experiment, in which reference materials were deposited on Anodisc filters and analyzed using the same FTIR imaging protocol (Figure S4).

Reference plastic materials were characterized using FTIR imaging under the same detection conditions to enable direct comparison with identified MPs in food samples. The cryo-milled polypropylene (PP) poweder were received originally as plastic pellets (Goodfellow GmbH, Hamburg, Germany) and milled in cryogenic condition by a mixer mill (MM 400, Retsch, Haan, Germany), which was then wet-sieved through 500 and 100 μm stainless-steel meshes sequentially to acquire a size range of 100-500 μm, with D_{50} size of 494 μm. Polyethylene (PE, BAM-P201) and polyethylene terephthalate (PET, BAM-P206) MP powder were acquired from German Federal Institute for Materials Research and Testing (BAM), with D_{50} size of 61.2 and 62.6 μm, respectively. Polyamide (PA) powder has a size of 25-30 μm (Goodfellow, Cambridge Limited). Polystyrene (PS) microspheres have sizes of 20 μm (ThermoScientific NIST traceable standards, CA, USA). Polymethyl methacrylate (PMMA) microspheres have a size of 27-32 μm (Cospheric, Santa Barbara, CA, USA). These reference materials span a range of common synthetic polymers and particle sizes, facilitating reliable spectral matching during FTIR analysis of environmental microplastics.

2.4 Method validation

2.4.1 QA/QC

Quality assurance and quality control in the laboratory followed a plastic-free rule. Glassware was utilized and replaced for plastic equipment whenver possible. Chemicals were filtered using either 0.2 µm cellulose acetate filters (Ø = 47 mm, Satorius) or 0.7 µm glassfiber filters (Ø = 47 mm, Whatman GF/F) before usage. Operators always wores cotton lab coats. Blank values were not extracted from any food samples. Each identified PP spectrum was double-checked. Other contamination sources from the consumables or devices are listed in Table S4.

2.4.2 LoD/LoQ

The limit of detection (LoD) and limit of quantification (LoQ) were determined using two methods. Method A calculates from the blanks, and Method B involves spiking low concentrations of MPs to determine if detection and quantification at these levels are possible.

Method A: Procedural blanks were prepared using 20 mL Milli Q water, and subjected to the same digestion SOPs for milk, TM and OJ for FTIR imaging. The MPs present in blanks, along with the LoD/LoQ for each matrix, were calculated. The LoD and LoQ were determined using the mean (µ) and standard deviation (σ) of the blanks, according to Equations 1 and 2, respectively:

$$LOD = \mu + 3 \times \sigma_{Blank} \quad \text{Eq. 1}$$

$$LOQ = \mu + 10 \times \sigma_{Blank} \quad \text{Eq. 2}$$

Method B: Polystyrene (PS) MPs with size of 20 µm (Sigma Aldrich, 2% solids) were selected for spiking because they can be differentiated from MPs in milk samples due to their spherical shape. The authenticity of PS was confirmed using IR spectra. The selected milk samples were control samples without any treatment packaged in glass bottles, with 1 mL milk serving as the matrix. Two concentration groups were spiked in triplicates (n = 3) at 100 and 1 µg/mL. The spiked samples were summarized in Table S5. Based

on the spiked concentration, LoD of the FTIR imaging workflow has a lower limit of 1 µg/mL, and an upper limit of 100 µg/mL (Figure S6).

2.4.3 Recovery

PP was the target polymer to understand the release from food packaging. The recovery rates of the sample preparation workflow were determined by spiking known amounts of PP into control samples of the three types of food matrices (n = 3), and comparing the resulting number of MPs identified with the number of MPs detected from neat plastics spiked onto an Anodisc filter. For each sample, 400 µg of PP powder was spiked as this amount was experimentally feasible to weigh accurately using an analytical balance for such low amount of MP powder. The samples for recovery rates were digested and analyzed by FTIR imaging, as described in Section 2.3.

2.5 Statistical analyses

Kruskal Wallis ANOVA was used to understand the difference of MP concentrations among various treatment groups, followed by Dunn's test on the mean between variables ($\alpha = 0.05$). Two sample t test was applied to compare the difference between heat treatment, packaging and storage time groups ($\alpha = 0.05$). Chemometric analyses including principal component analysis (PCA) and hierarchical cluster analysis (HCA) were applied to cluster IR spectra of MPs and of food matrices.

3. Results

3.1 Established standard operation protocols (SOPs) for digesting food samples

The most effective SOPs developed for three types of food samples are outlined in Figure 2. The selection of SOPs considered compatibility to the existing FTIR imaging set-up and the digestion effects of

complex matrices. For milk samples, 20 mL is pipetted into a 50 mL glass flask with a glass lid. Chemical digestion involves the use of potassium hydroxide (10% w/v KOH). On the first day, 10 mL of 10% KOH solution is added to the milk sample, which is then digested in a shaker/incubator at 37 °C and 100 rpm for 24 h. On the second day, an additional 10 mL of 10% KOH is added, and digestion continues for another 24 h. Following digestion, the milk sample is filtered through a 10 μm stainless steel mesh (Ø = 25 mm) using a vacuum filtration system. The particles are subsequently rinsed from the mesh with Milli Q water and ethanol into a 50 mL beaker, which is then covered with aluminum foil and sonicated for 5 min to remove any remaining particles from the mesh. The suspension is then filtered through an Anodisc filter (pore size 0.2 μm, Ø = 25 mm). The Anodisc filter is then stored in a glass petri dish and dried in an oven overnight at 30 °C for FTIR imaging.

For tiger nut milk, 20 mL TM is pipetted into a 50 mL glass flask with a glass lid. TM sample is digested with 10 mL of 10% KOH for 24 h in a shaker/incubator at 37 °C and 100 rpm. On the second day, the digested TM is added with another 10 mL of 10% KOH and digested for another 24 h. On the third day, the digested TM is filtered over a 10 μm stainless steel mesh. If the mesh is blocked, replace it with another mesh until all the digested TM is filtered. The meshes with particles are rinsed off with Milli Q water and ethanol to a beaker, and 10 mL 30% H_2O_2 is added to the beaker. The beaker is then sonicated for 5 min to further remove particles from the meshes, and digested mixture is incubated in a shaker/incubator at 37 °C at 100 rpm for 24 h. On the fourth day, the mesh is filtered over an Anodisc filter (pore size 0.2 μm, Ø = 25 mm), collected in a glass petri dish and dried at 30 °C for FTIR imaging.

For orange juice, 20 mL of OJ is pipetted to a 50 mL glass flask with a glass lid. Five mL of cellulase and 20 mL NaOAc buffer are added to the OJ sample to digest it for 24 h in a shaker/incubator at 50 °C and 100 rpm. On the second day, 20 mL of UTS mixture is added to the OJ sample, and a magnetic stirrer is also added to the flask. The OJ sample is frozen at -20 °C for 40 min until crystal formation, and then digested on a magnetic stirrer at room temperature for 24 h. After digestion on the third day, the OJ sample is first filtered over a 10 μm stainless steel mesh. In case of blockage, additional meshes can be used to filter all the sample. The particles on the mesh are rinsed off into a beaker and sonicated for 5 min.

The beaker is added with 10 ml of 30% H_2O_2 and oxidized for 24 h in a shaker/incubator at 37 °C and 100 rpm. On the fourth day, the sample is filtered over an Anodisc filter (pore size 0.2 μm) for FTIR imaging. Recipes for preparing chemical mixtures and buffer are provided in Table S6. The effect of digestion using established SOPs on milk, tiger nut milk and orange juice is shown in Figure 2.

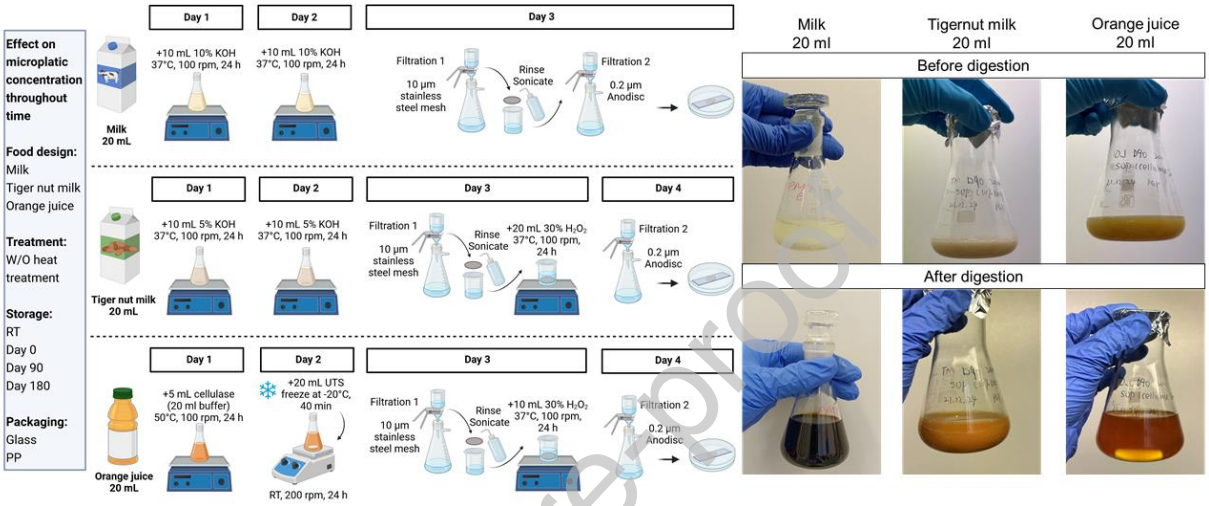

Figure 2. Established standard operating protocols (SOPs) used to digest milk, tiger nut milk and orange juice for MP analysis using FTIR analysis to study the effect of food design, treatments, storage, and packaging on MP concentration over time. Photos of digestion results of the three types of food before and after digestion are included. Created with BioRender.com.

3.2 Method validation

Performance of the particle identification algorithm, the Purency software was evaluated by spiking 6 types of MPs on the Anodisc filters for FTIR imaging. The algorithm correctly detected 100% of neat plastic polymers without misidentification (Figure S4). Given the accuracy of MP detection algorithms, a total of 18 samples were prepared for method validation (9 for blanks and 9 for recovery) using FTIR imaging. No MPs were detected in the procedural blanks of milk (n = 3), and the LoD/LoQ in milk is therefore 0/0 MP. In TM procedural blanks (n = 3), 1,1, and 0 MPs were detected, and the LoD/LoQ in

TM is 2/6 MP. The procedural blanks of OJ (n = 3) had 3, 3, and 3 MPs, and the LoD/LoQ in OJ is 3/3 MPs. IR images of the procedural blanks of 3 types of food is shown in Figure S5.

Samples for recovery rates were prepared by spiking 400 µg cryo-milled PP powder (D_{50} = 494 µm) into the control samples of milk, TM and OJ (n = 3), and were digested with the SOPs for FTIR imaging. The recovery rates were calculated by comparing the resultant number of PP identified in 3 types of food samples to the number of 400 µg PP powder. The recovery rate of milk digestion SOP was 66 ± 50%, TM SOP 38 ± 16%, and OJ SOP 98 ± 14%. This corroborates with visual inspection of the Anodisc filter after digestion, where TM filter had a filter cake deposited the Anodisc filter, and we did not visually observe any color changes on the Anodisc filters of the OJ samples.

3.3 MP variation throughout time under treatment, packaging and storage conditions

A total of 54 samples (3 types of food, 6 treatments per type of food, and each sample in triplicates) were digested and measured by FTIR imaging (Figure 3). PP-MPs identified in milk, TM and OJ averaged 3.5 ± 3.7, 1.6 ± 2.9, and 7.1 ± 7.0 n/20 ml, respectively (Figure 2a). There was a significant difference among the three types of food samples (Kruskal Wallis ANOVA, n = 52, p = 0.00103), and OJ was significantly different from TM. Within the three types of food groups, there was no significant difference among milk treatment groups. TM Glass D180 and TM PP D180 were significantly different from TM control, Glass D0, PP D0 and PP D90 samples. There was no difference among OJ treatment groups.

The total MP concentration in all food samples ranged from 0 - 24 n/20 mL milk, 0 - 10 n/20 ml TM, and 0 – 58 n/20 ml OJ. The average MP concentration in milk, TM and OJ were 7.4 ± 6.7, 3.5 ± 3.8, and 12.3 ± 13.7 n/20 ml, respectively (Figure 2b). Among the three types of food, total MP concentrations were significantly different (Kruskal Wallis ANOVA, n = 52, p = 0.00858), and OJ was significantly different from TM. Milk control samples without any treatment were already contaminated with MPs at an average of 10 ± 6 n/20 mL, and milk PP D180 had 5 ± 9 n/20 mL. TM control had 4 ± 5 n/20 mL, and TM PP

D180 reached 8 ± 2 n/20 mL. MPs in OJ control were at 17 ± 14 n/20 mL, higher than milk and TM control, and in OJ PP D180 reached 23 ± 30 n/20 mL.

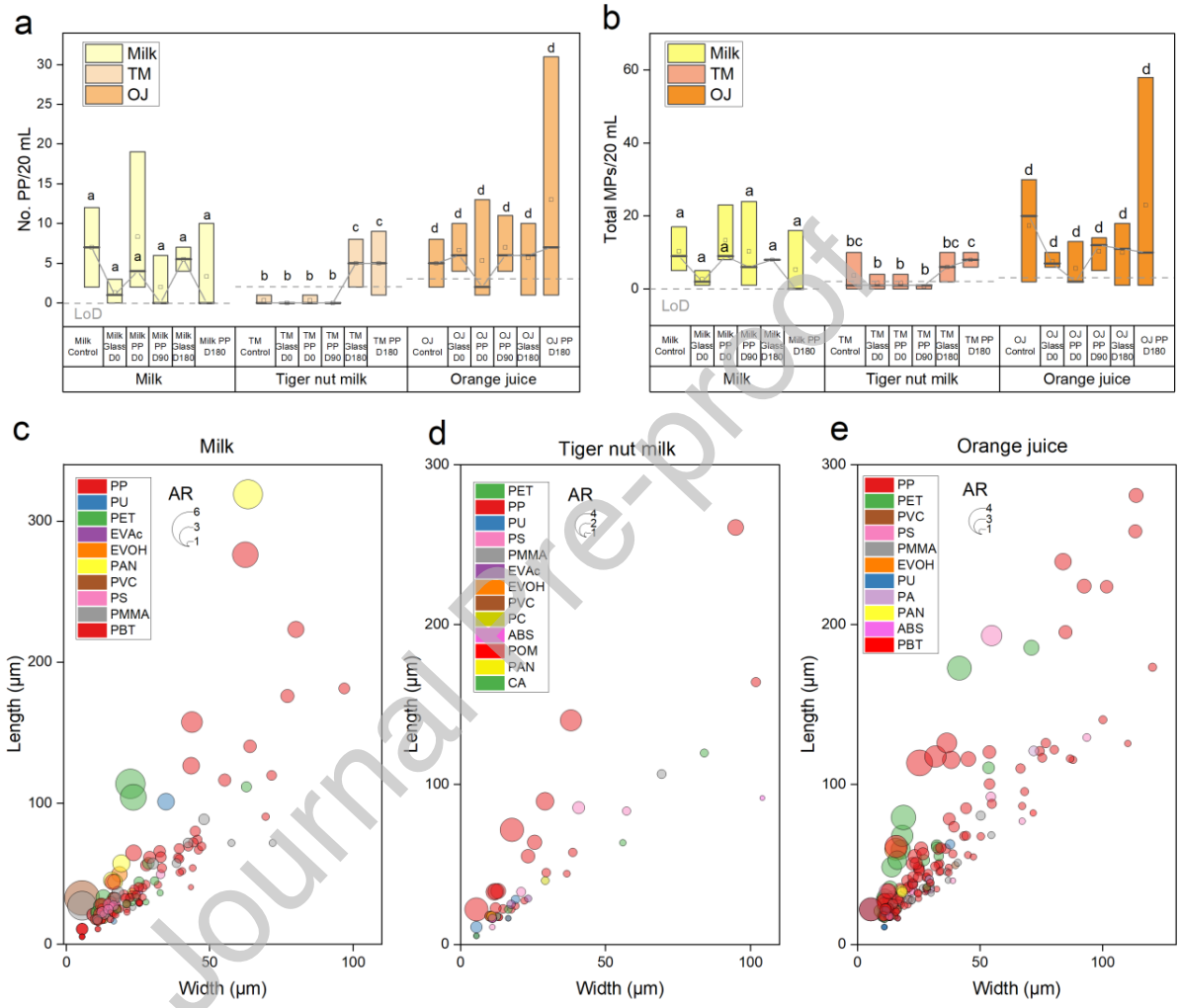

Figure 3. **Number concentrations of MPs in milk, tiger nut milk and orange juice samples under different packaging, treatment conditions, and storage time, and characteristics of all detected MPs including polymer type, length, width and aspect ratio.** MP concentrations were significantly different among three types of food samples (Kruskal Wallis ANOVA, n = 52, p = 0.0103 for No. PP and p = 0.00858 for total MPs). (a-b) Number concentrations of (a) PP MPs and (b) total MPs identified in milk, TM and OJ samples. The box shows the upper and lower quartile, the square shows the median, and the

thick line shows the mean. (c-e) Bubble plots on the length, width, AR and polymer types of all identified particles in (c) milk, (d) TM and (e) OJ samples. AR: aspect ratio.

Between control and heat treatment groups of the three types of food samples (i.e., glass control vs glass D0 of all three types of food), there was no significant difference between the number of PP MPs before and after heat treatment groups of 3 types of food samples (two-sample t test, $p = 0.438 > 0.05$) or total MP particles ($p = 0.088$). Between D180 Glass and PP packaging groups of the three types of food samples, there was no significant difference for PP concentration ($p = 0.53$) nor for total MP concentration ($p = 0.48$). Among the three storage condition groups of the three types of food (D0 and D180), there was no significant difference for PP concentration (Kruskal Wallis ANOVA, n = 44, $p = 0.25$) nor for total MP concentration ($p = 0.27$).

Characteristics of each identified MP particles are illustrated in Figure 3c-d, showing that the most common MP polymer type was PP, and 86% of all MPs detected in three types of food were < 100 μm, and 69% of MPs were < 50 μm. Size and shape distributions of total MP particles detected from FTIR chemical images in milk samples from D0 and D180 were further visualized by length, width and aspect ratio (Figure S8).

In all milk samples, 55% of MPs were found in PP bottles, and 45% MPs were detected in glass bottles. PP was the most abundant polymer (57%), followed by polyethylene terephthalate (PET, 12%), poly(methyl methacrylate) (PMMA, 11%), polyacrylonitrile (PAN, 8%), polystyrene (PS, 5%) and polyurethane (PU, 3%). The size of MPs decreased from an average of 70 ± 93 μm at Day 0 to 39 ± 38 μm at Day 180, and the difference was significant (two-sample t test, $p = 0.02 < 0.05$). Particle width also decreased from 34 μm to 25 μm, but the difference was not significant between particle width at Day 0 and Day 180 ($p = 0.10$). The aspect ratio (AR) of MPs at Day 0 and Day 180 was significantly different ($p = 0.007 < 0.05$), which decreased from 1.86 (0.94) at Day 0 to 1.49 (0.44) at Day 180. PET was dominated by fibers (aspect ratio > 3, Figure 2c), indicating general contamination from ambient environments with synthetic fibers during the food production.

In all TM samples, the length of MPs at Day 0 differed significantly from Day 180 (two sample t test, p = 0.028). The average length at Day 0 was 30 ± 30 µm, and increased to 74 ± 104 µm at Day 180. The median length increased from 18 µm at Day 0 to 30 µm at Day 180. Most of the length of MPs was within the range 0 – 20 µm (42%), followed by 20 – 50 µm (29%), 50 – 100 µm (15%) and >100 µm (14%). Polymer types were dominated by PP (46%), PS (14%) PET (8%) and PU (8%).

In all OJ samples, the length of detected MPs differed significantly between Day 0 and Day 180 (two sample t test, p = 0.020). The mean length of MPs decreased from 67 ± 89 µm at Day 0 to 44 ± 36 µm at Day 180. The median length was 34 µm at Day 0 and 33 µm at Day 180. The majority has a length ranged from 20 – 50 µm (45%) and <20 µm (23%). Particles with a length 50 – 100 µm and >100 µm comprised 17% and 15%, respectively. The predominant polymer type in all OJ samples was PP (58%). Other polymers identified included PET (12%), PMMA (11%) and PS (5%).

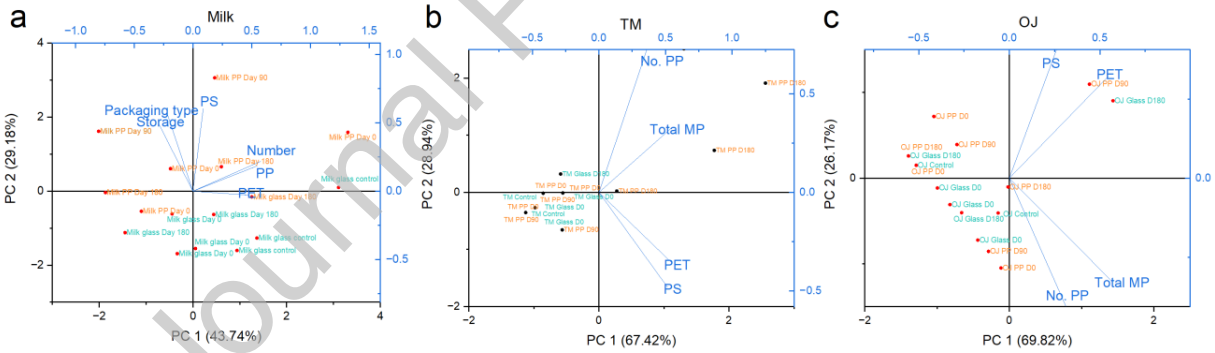

Figure 4. Principal component analysis on the MP concentrations with variables including packaging, storage, and polymer types. For milk samples, the PC2 explained the variation of MPs due to packaging (PP packaging marked in orange and glass packaging marked in green).

Principal component analysis (PCA) was further employed to understand the potential influencing factors on the MP variation in milk, TM and OJ (Figure 4). For milk, the variation in MPs can be explained by

PC1 and PC2, with packaging being a key factor. PC 1 accounted for the variation of the MP concentration with the detection of PP and PET, and PC 2 was positively correlated with glass and PP packaging, further supporting the influence of ambient air contamination (detection of PET fiber and PS). Similar to milk, the contamination from ambient air was also evident in TM and OJ samples, as indicated by PC2 (Figure 4b-c). However, the influence of storage time was not clearly defined by the PCA. Despite low MP concentrations detected in milk samples, plastic packaging and ambient environment were identified as sources of MPs in milk, TM and OJ samples.

3.4 Chemical fingerprints of microplastics identified in food samples

The Anodisc filter was chosen as the substrate for FTIR imaging in transmission mode. The organic matrix in food samples posed challenges for the identification of plastic polymers. Even after digestion of milk, the Anodisc filter was covered with a layer of white/beige organic matter, occasionally resulting in a filter cake. The IR bands from milk and tiger nut milk were dominated the entire scanned area. The interference from the spectra of the matrix, attributed to C-H bonds in the functional group region, caused most identified plastic spectra to display both the functional groups of the polymer and the matrix, with increased intensity of C-H bands in the 2900 - 3000 cm^{-1} region compared to the reference materials (Figure 4). Nevertheless, PP, PS, PET, PAN and PVC can still be accurately identified based on the characteristic bands in the fingerprint region.

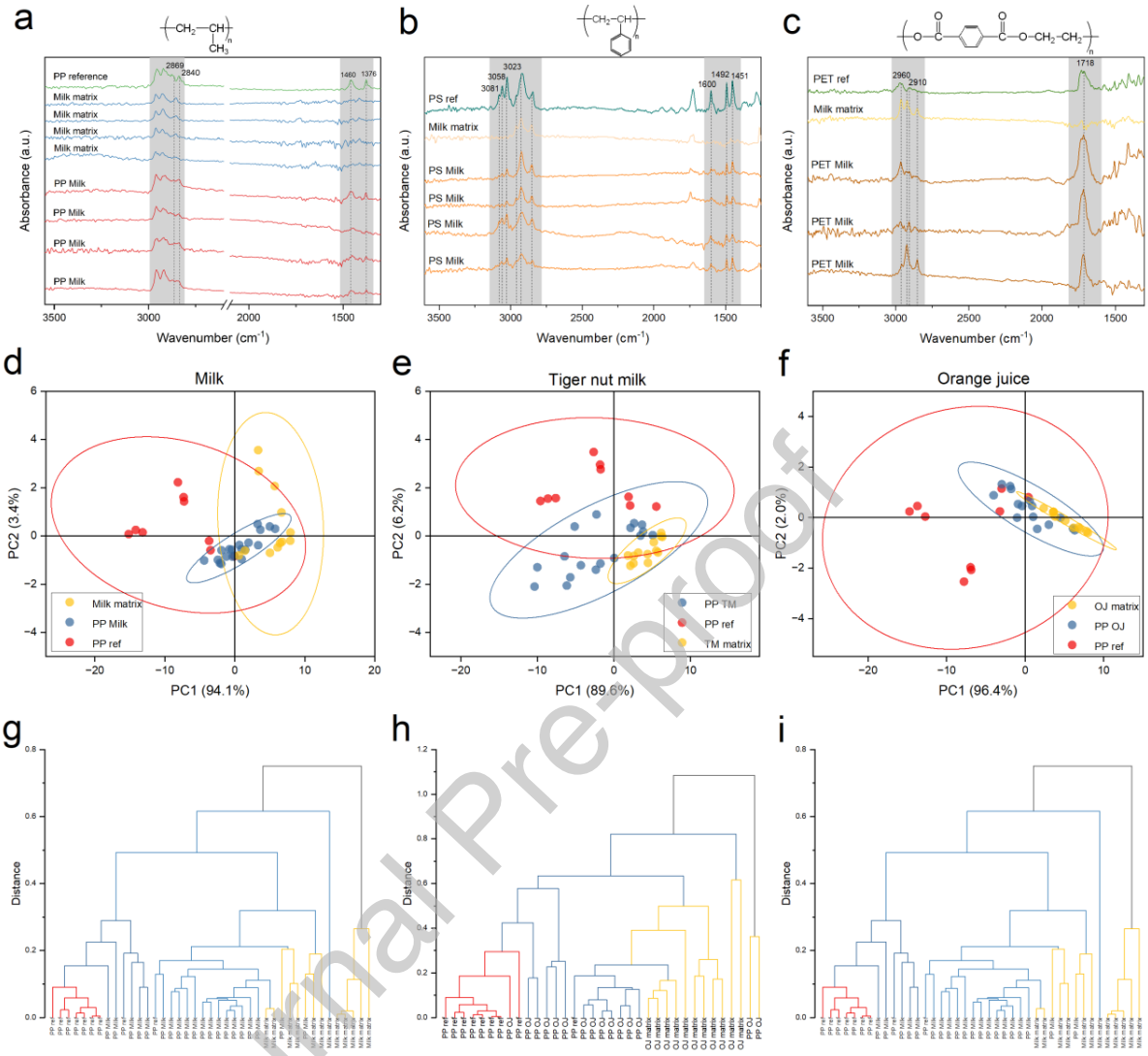

Figure 5. Matrix effect on the IR spectra of identified MPs in food. (a-c) Representative IR spectra of (a) PP, (b) PS and (c) PET reference materials. MPs and milk matrix show the difference in characteristic bands in fingerprint regions, and interference from matrix of remaining organic matter (C-H bond in 2900-3000 cm^{-1} region) that also appeared in the functional group regions of PP, PS and PET detected in milk. (d-i) Chemometric analysis of the IR spectra of reference PP material, 3 types of food matrices and PP identified from the 3 types of food samples. (d-f) Principal component analysis of IR spectra of PP reference materials (marked in red dots), PP identified in food samples (marked in blue dots) and spectra of food matrix (marked in yellow dots). The IR spectra of PP MPs identified in food matrices show the

overlap of those with PP reference material and pure food matrices, indicated by the 95% confidence ellipses. (d) Milk, (e) TM, (f) OJ. (g-i) Hierarchical cluster analysis of IR spectra of PP reference materials (red), PP identified in food (blue), food samples and milk spectra (yellow), showing the overlap of the IR spectra of PP identified in food with those of PP reference materials and food matrices. (g) Milk, (h) TM (i) OJ.

PP spectra is characterized by the CH_3 bending at 1,460 and 1,376 cm^{-1} (Smith, 2021). Characteristic IR bands of PS include the aromatic C-H stretching at 3,081, 3,058 and 3,023 cm^{-1}, as well as the aromatic ring modes at 1,600, 1,492 and 1,451 cm^{-1} (Olmos et al., 2014). The IR spectra of PET is characterized by a very strong band at 1,718 cm^{-1}, assigned to the stretching of C=O of carboxylic acid group (Chen et al., 2012). C-H symmetric stretching at 2,960 and 2,910 cm^{-1} has medium to weak bands, which may overlap with the C-H stretching bands of the organic matrix. PS can be identified with aromatic stretching at 3,081, 3,056 and 3,023 cm^{-1}, as well as 1,600 and 1,492 cm^{-1} assigned to the aromatic ring modes (Fang et al., 2010). However, PE and PA spectra cannot be differentiated from lipids and proteins, which are more dominant in milk and TM samples. Therefore, PE and PA could not be attributed to synthetic or natural sources from IR spectra and were not included in the results.

PCA was used to further interpret the matrix effect on IR spectra of MP reference materials, MPs detected in food and food matrices (Figure 5d-f). For milk, score plots of IR spectra of PP reference material, PP in food samples and food matrices shows that PC1 explained 94.1% of the variability, and PC2 explained 3.4% of viariability. The significant bands in PC1 loadings are the 2,954, 2,869, 2,842 cm^{-1}, which denotes CH_2 stretching in the funtional groups region of lipids and plastics, as well as wavenumbers at 1,457, 1,377 cm^{-1}, which denotes CH_3 symmatrical bending of PP. For TM, PC1 and PC2 explained 89.6% and 6.2% of the variability, respectively. PC2 loading of TM is characterized by positive values of bands at 2,962, 2,873, 2,838, 1,458, and 1,370 cm^{-1}, and negative values in the wavenumbers 3000-3500 cm^{-1}, denoting the functional groups of carbohydrates. Unlike milk which is clustered by PC1, both PC1 and PC2 explained clusters of TM. For orange juice, PC1 explained 96.4% of the variability, with PC1 loadings denoting characteristic bands of PP.

Dendrograms of HCA (Figure 5g-i) show not only the clusters of PP reference materials (marked in red), PP identified in food matrices (marked in blue), food matrices (marked in yellow), but also the overlap between PP reference materials and PP identified in food, and the overlap between PP identified in food and food matrices for milk, TM and OJ.

3.5 Human body burden of MPs via food intake

To estimate the body burden of MPs via three types of food ingestion in the European Union (EU-27) for the year 2023, we use annual consumption per capita values and assume average MP concentrations in the respective foods. The total consumption of milk was 1.465×10^{11} kg, while the consumption of orange juice was 5.42963×10^{8} kg (Indexmundi, 2024). Assuming densities of 1.035 and 1.038 kg/L, for milk and orange juice, and EU population of 449.2 million (EC, 2024), the annual consumption per capita are 315 and 1.16 L for milk and orange juice. Plant milk consumption in Germany was 3.8 kg per capita (Milk-food, 2023). This leads to yearly MP exposures of $1.2\times10^{5} \pm 1.1\times10^{5}$, $6.8\times10^{2} \pm 7.2\times10^{2}$, and $7.2\times10^{2} \pm 7.9\times10^{2}$ MPs per capita per year through milk, plant milk and orange juice consumption, respectively. These calculations provide a rough estimate of the annual microplastic intake via milk, plant milk, and orange juice consumption in the EU-27.

4. Discussions

Comparison with other studies in food samples and human body burden

With the increasing concern about MNPLs and human health, and the potential significant health effects via food and beverages, an increasing number of studies have found alarming levels of microplastics in food and beverage products and its packaging, which have utilized mostly spectroscopic methods for microplastic identification and quantification (Da Costa Filho et al., 2021; Li et al., 2020). Table 4 lists the MP concentration detected in milk or milk products to date. The detected MP concentrations in milk from

our study ranked average among all reports. Compared to the study with the highest concentration, confocal Raman microscopy applied in that study has a detection limit down to 1 μm. In our study, FTIR imaging has a detection limit of 11 μm, and their pretreatment steps (digestion, filter types) and Raman spectroscopy enabled the detection of smaller particles around 5 μm. The lowest MP concentration reported is two orders of magnitude lower than that in our study, however, their analytical workflows had a much higher size detection limit (> 100 μm) compared to FTIR imaging, with their sample volume up to 1 L compared to 20 mL. MPs in milk powder detected by the same FTIR imaging technique showed MP concentration in a similar order of magnitude and size ranges as those in our study, where the authors also pointed out that the milk powder itself had low MP exposure to infants compared to the release of MP from the feeding bottle for milk powder preparation, with 6.8 times higher risk of exposure (Zhang et al., 2023). The omnipresence of MPs in beverages were also reported recently. In beverages including bottled water, soft drinks, beer and wine sold in France, the majority of MPs detected has size ranges from 50 – 100 μm detected sing μATR-FTIR. Glass bottles, on the contrary, contained highest MPs up to 83 n/L in beer, likely due to the release from the cap coated with alkyd thermosetting resin (Chaïb et al., 2025). In our study, the PE cap was sealed with a piece of aluminum foil, preventing the potential release of MPs while twisting the cap.

Estimation of human exposure to MPs via food suggested a higher intake from milk compared to plant milk and orange juice, which is still at a similar order of magnitude compared to previous studies. Mohamed Nor et al. (2021) estimated that exposure via milk consumption was circa 1.1×10^3 MPs per capita per year, while Jeffries et al. (2025) quantified MPs using py-GC/MS and suggested intake via beverages was 1.7 – 2.0 mg per capita per year, with tap water being the greatest contributor. Domenech and Marcos (2021) estimated that body burden from bottled water reached 9.89×10^9 and from seafood was 2.2×10^3 MPs per capita per year. Zhang et al. (2020) estimated that exposure via seafood was at a similar range of $0 – 1.3 \times 10^4$ MPs per capita per year. MP exposure via milk, plant milk and orange juice was less significant in contrast to water and air (Mohamed Nor et al., 2021; Zhang et al., 2020), but may potentially induce health effects due to interaction with nutrients in food (Kaseke et al., 2023). Upon

exposure to intestinal epithelial cells, microplastics can form protein corona, disrupting intestinal barrier and induce oxidative stress (Brouwer et al., 2025). *In vitro* or *in vivo* studies confirmed that exposure induced cell apoptosis, and have genotoxicity and cell toxicity effects, leading to diseases and disturbances in gut microbiota (Winiarska et al., 2024). Milk with a higher body burden of $1.2\times10^5 \pm 1.1\times10^5$ per capita per year should be the major focus in mitigating human exposure via food intake.

Table 4. Comparison of results of MPs in milk products in the present study with other published studies.

Sample type	Sample volume	Analytical method	Digestion protocol	MPL concentration	Polymer type	MPL size	References
Branded milk from Turkey	1 L	ATR-FTIR	N/A	6 ± 5 n/L	nylon-6, PET, EVA, PP, PU	25–5050 µm	Basaran et al. (2023)
Branded milk from Mexico	1 L	Micro-Raman	N/A	1 - 14 n/L	Polyethersulfone (PES), polysulfone (PSU)	0.1–5 mm	Kutralam-Muniasamy et al. (2020)
Skimmed milk from Ecuador	500 mL	FTIR	Oxidation	16 – 53 n/L	HDPE, LDPE, (polyacrylamide) PAM, PP	28.45–2329.41 µm	Diaz-Basantes et al. (2020)
Raw milk and powdered milk from Switzerland	25 mL of raw milk and 25 g of powdered milk	Micro-Raman and SEM-EDX	Enzymatic and chemical digestion	204 - 1004 n/100 mL	PE, polyester, PP, polytetrafluoroethylene (PTFE), PS	5 – 7 µm (surface area 50 μm^2)	Da Costa Filho et al. (2021)
Infant milk powder from China	100 g	FTIR imaging	Enzymatic and chemical digestion	4 ± 3 n/100 g	PE, PET, PP, PA, PVC	139 ± 343 µm	Zhang et al. (2023)
Infant formulas	10 g	Micro-Raman	Oxidation	42 ± 27 MPs/100 g	PA, PE, PP, PET	10-5000 µm	Kadac-Czapska et al. (2024)
Cow milk from Spain after various treatment, packaging and storage conditions	20 mL	FTIR imaging	Alkaline digestion	5 ± 6 n/20 mL	PP, PET, PS, PAN, PVC	11 – 495 µm	This study

Complex organic matrices for MP analysis and digestion methods

Digestion of milk, powdered milk or human breast milk for MP analysis is key to successfully detecting of MPs in food, and some protocols have been established to remove complex organic matrices (Da Costa Filho et al., 2021). Those that reported lower concentration lacked digestion and missed out the smaller MP fraction < 50 µm (Kutralam-Muniasamy et al., 2020). For milk and powdered milk, every 25 g milk powder or 25 mL milk liquid subjected to enzymatic digestion by adding 2 mL multi-enzymatic detergent and filtered over a 5 µm silicon filter for Raman analysis (Da Costa Filho et al., 2021). For breast milk,

every 4 g breast milk was digested with 10% KOH at 40 °C for 48 h and filtered through a 1.6 µm Whatman GF/A filter membrane for Raman analysis (Ragusa et al., 2022). Commercial powdered milk (100 g) was digested with artificial gastric acid and pancreatic enzymes, and the digestate was filtered over 8 µm polycarbonate filters for FTIR imaging (Zhang et al., 2023). Infant formulas from various brands (10 g) were mixed with 70 mL of Milli Q water and digested with 50 mL of 30% H_2O_2 at 60 °C for 8 h until coagulation occurred, and was visually inspected by light microscopes, followed by Raman analysis on each inspected particle (Kadac-Czapska et al., 2024). When working with complex matrices, the most important aspect to consider is the cost-effectiveness of pre-treatment for successful detection of particles at relatively low concentrations.

In our study, we adopted the alkaline digestion method for milk that proved effective for digesting tissue samples (Pfeiffer and Fischer, 2020). It is effective for filtering a volume up to 100 mL of milk. For TM samples that are rich in carbohydrates, we tested oxidation (H_2O_2, NaClO), alkaline digestion and enzymatic digestion at various concentration, temperatures and digestion environments. We found that only when the 10% KOH (w/v) was added over two consecutive days will prevent the formation of a very viscous solution that could not be filtered over the stainless steel mesh. For orange juice that has fibers and could not be directly filtered, a combination of cellulase and dissolution using UTS proved successful in removing fibers for filtration with no filter cake formation. Filter cake is challenging for some particle detection method based on particle image analysis, e.g., Laser Direct Infrared Imaging (LDIR) or Raman ParticleScout, particularly when the matrix is not completely removed. These particle image-based methods can be faster when no visible particles can be observed under microscopes, but may fail to detect particles that are not visible under microscopes due to the presence of a complex matrix. However, workflows based on FTIR imaging, as applied in this study, can overcome this issue for successful particle identification even in the presence of filter cakes.

FTIR and other analytical methods available for food matrices

Although the interference from organic matrix remains a challenge for the FTIR technique and subsequent identification of MPs, the transmission mode provides an advantage that particles can still be detected even when they are not visible from the optical image due to their small size or coverage by the organic matrix, as demonstrated by the detected PP particles in milk (Figure S7). Albeit the relatively high recovery rates and detection limits, complex matrices like TM resulted in the least recovery rate, which on the one side leads to underestimation of MPs in food. This is because of the overlap between the food matrix and spectra. On the other side, organic matter may be misidentified as plastics, e.g., lipids as PE, which may lead to false positive. They reduce the high sensitivity of FTIR imaging and machine-learning based workflow for quantification. Another disadvantage of FTIR imaging is the long scanning duration and excess data from the background scanned. One sample takes 6 hours to finish scanning. The machine-learning based algorithm takes several days to finish one sample analysis on the servers.

Mass-based methods, such as pyrolysis-GC/MS, are also used for detecting MPs in milk and other complex food samples in the food basket study (Jeffries et al., 2025). There, concentrations of MNPLs were extremely low in 1 g of freeze-dried samples, indicating that mass-based quantification methods are not suitable for routinely analyzing large volumes of food samples with detected concentrations below the LoD in most samples. In addition, even with a detection limit of 11 µg/g for PP, the microplastic fractions (>1 µm) are missing from most dairy food samples (skimmed milk, cheese, eggs, yogurt), and nanoplastic fraction (0.3 – 1 µm) is challenging due to the high MNPL concentrations detected in blank controls from plastic equipment used during solvent extraction and general lab contamination. These challenges call for more sensitive methods for detecting MNPLs in complex food samples using number- and mass-based concentrations.

Food packaging contribution to MP concentration in food

The melting temperature of plastics materials used for packaging can be similar to the temperature used during thermal treatment (e.g., LDPE at 110 ˚C), packaging was thus hypothesized to contribute to MP variation in food. However, MP concentration in three types of food did not increase significantly during

180 days of storage at room temperature. There was no significant difference between glass and PP packaging. The presence of polymer types other than PP in the food samples indicated general MP contamination from the ambient air during food processing. While the heat treatment may restructure the plastic polymer chains, PP has a melting temperature of 170 °C and should resist the thermal treatment at 121 and 100 °C used in the present study. Common heat treatment methods include high-temperature, short-time pasteurisation (HTST), ultra-high-temperature processing (UHT) and sterilization. HTST pasteurisation of liquid milk at 72 °C for 15 – 20 s has a shelf life of 5 – 10 days refridgerated. Extended shelf life (ESL) milk has a longer shelf life of 14 – 28 days, which is addtional treated with either non-thermal processes, or thermal processing at 127- 135 °C for 0.5 – 3 s to remove bacteria and spores (Rauh and Xiao, 2022). UHT milk has a shelf life of 3 – 12 months due to the inactivation of most mesophilic and thermophilic spores, while that of sterilized milk reaches up to 12 – 24 months. The former is treated at 135 – 141 °C for 3 - 6 s, while the latter is heated at 121 °C for 20 min (Rauh and Xiao, 2022). However, in the present study, heat treatment did not have a significant impact on MP concentraiton in milk, TM or OJ.

The observed factors that influenced MP concentration were food type, where acidic orange juice had the highest MP concentrations, as well as a sligh influence from packaging. In a study that quantified MP release into beverages from disposible cups, acidic carbonated beverages enhanced five times MP release than ultrapure water (Chen et al., 2023). Similarly, in the food basket study (Jeffries et al., 2025), PET was only detected in one bottled water samples packaged in PET bottles among all tap water, bottled water, beer and wine samples, proving the source of MNPLs from plastic packaging. The observation of a decreasing size of PP detected in milk throughout time and the small size of most particles below 50 μm may indicate a further fragmentation from polymers to oligomers or monomers. Oligomers can also migrate into milk and dairy products, as evidenced by studies using food (including milk) and food simulants to understand the migration of oligomers from PFCMs of styrene-acrylonitrile-copolymer (SAN) and acrylonitrile-butadiene-styrene-copolymer (ABS) (Kubicova et al., 2022), and PA 6 and PA66 (Canellas et al., 2021). Acidic environments can faciliate hydrolytic degradtion of PE into MPs during

oxidation (Ariza-Tarazona et al., 2020). Plastic particles at nano-sized range can interact with milk protein and lipids, leading to coalescence and the formation of large protein-MP or lipid-MP heteroaggregrates, which can decrease the bioavailability of nutrients in milk. This can alter milk digestion processes, and influence glucose digestion via decreased amylase activity (Kaseke et al., 2023). However, studies on mechanisms of MP interactions with nutrients and their respective health effects on humans, especially infants and elderly people, are critically lacking.

5. Conclusions

This study systematically investigated microplastic concentrations in complex food matrices under various food design, treatment, packaging and storage conditions prior to consumption. To minimize matrix effect and enable accurate microplastic detection and quantification, matrix-specific digestion protocols were established using a combination of chemical digestion, enzymatic digestion and oxidation methods, allowing reliable sample preparation for FTIR imaging. Polypropylene (PP) was the most frequently detected polymer, and most particles were below 50 µm. Among all factors tested, the main factors which had significant impact on the MP concentrations are the food type (acidic orange juice) and packaging (PP). In contrast, heat treatment (UHT) and storage time (up to 180 days) showed minimal impact on MP variation. Of the three types of food investigated, milk contributed the highest estimated body burden at $1.2\times10^5 \pm 1.1\times10^5$ particles per capita per year, highlighting the need for targeted mitigation measures to reduce human exposure. The limitations of the current study is that due to the complexity of the matrices and the instrumentation, extraction and identification of microplastics below 11 µm remained challenging. Future research should prioritize establishing matrix-specific digestion protocols suitable for analyzing the sub-micron size fractions of micro(nano)plastics, which are especially relevant for long-term human exposure and health risk assessment.

Acknowledgement

This study is funded by the EU Horizon 2020 project PLASTICHEAL (GA: 965196). We thank Shweta Singh and Ahmed Reda Abdulaziz for the assistance with sample preparation and analysis.

References

Alvarez, V.B. and Pascall, M. (2011), pp. 16-23, Academic Press, San Diego, CA, USA.

Amador-Espejo, G.G., Suarez-Berencia, A., Juan, B., Barcenas, M.E. and Trujillo, A.J. 2014. Effect of moderate inlet temperatures in ultra-high-pressure homogenization treatments on physicochemical and sensory characteristics of milk. J Dairy Sci 97(2), 659-671.

Ariza-Tarazona M. C., Villarreal-Chiu J. F., Hernández-López J. M., De la Rosa J. R., Barbieri V., Siligardi C., Cedillo-González E. I., Microplastic pollution reduction by a carbon and nitrogen-doped TiO2: Effect of pH and temperature in the photocatalytic degradation process, Journal of Hazardous Materials, 395, 2020, 122632,

Basaran, B., Özçifçi, Z., Akcay, H.T. and Aytan, Ü. 2023. Microplastics in branded milk: Dietary exposure and risk assessment. Journal of Food Composition and Analysis 123.

Brouwer H., Busch M., Yang S., Venus T., Aalderink G., Crespo J. F. F., Villacorta A., Hernández A., Estrela-Lopis I., Boeren S., Bouwmeester H., Toxicity of true-to-life microplastics to human iPSC-derived intestinal epithelia correlates to their protein corona composition, Journal of Hazardous Materials, 495, 2025, 138908,

Canellas, E., Vera, P., Song, X.C., Nerin, C., Goshawk, J. and Dreolin, N. 2021. The use of ion mobility time-of-flight mass spectrometry to assess the migration of polyamide 6 and polyamide 66 oligomers from kitchenware utensils to food. Food Chem 350, 129260.

Chaïb, I., Doyen, P., Merveillie, P., Dehaut, A. and Duflos, G. 2025. Microplastic contaminations in a set of beverages sold in France. Journal of Food Composition and Analysis 144, 107719.

Chen, Z., Hay, J.N. and Jenkins, M.J. 2012. FTIR spectroscopic analysis of poly(ethylene terephthalate) on crystallization. European Polymer Journal 48(9), 1586-1610.

Chen H., Xu L., Yu K., Wei F. and Zhang M., Release of microplastics from disposable cups in daily use, Science of The Total Environment, 854, 2023, 158606,

Codina-Torrella, I., Gallardo-Chacon, J.J., Juan, B., Guamis, B. and Trujillo, A.J. 2023. Effect of Ultra-High Pressure Homogenization (UHPH) and Conventional Thermal Pasteurization on the Volatile Composition of Tiger Nut Beverage. Foods 12(4).

Da Costa Filho, P.A., Andrey, D., Eriksen, B., Peixoto, R.P., Carreres, B.M., Ambuhl, M.E., Descarrega, J.B., Dubascoux, S., Zbinden, P., Panchaud, A. and Poitevin, E. 2021. Detection and characterization of small-sized microplastics (>/= 5 microm) in milk products. Sci Rep 11(1), 24046.

Diaz-Basantes, M.F., Conesa, J.A. and Fullana, A. 2020. Microplastics in Honey, Beer, Milk and Refreshments in Ecuador as Emerging Contaminants. Sustainability 12(14).

Dileepan, A.G.B., Jeyaram, S., Arumugam, N., Almansour, A.I. and Santhamoorthy, M. 2025. Identification and occurrence of microplastics in drinking water bottles and milk packaging consumed by humans daily. Environ Monit Assess 197(3), 261.

Domenech, J. and Marcos, R. 2021. Pathways of human exposure to microplastics, and estimation of the total burden. Current Opinion in Food Science 39, 144-151.

EC 2024 Population and population change statistics.

Fang, J., Xuan, Y. and Li, Q. 2010. Preparation of polystyrene spheres in different particle sizes and assembly of the PS colloidal crystals. Science China Technological Sciences 53(11), 3088-3093.

Foroutan, A., Guo, A.C., Vazquez-Fresno, R., Lipfert, M., Zhang, L., Zheng, J., Badran, H., Budinski, Z., Mandal, R., Ametaj, B.N. and Wishart, D.S. 2019. Chemical Composition of Commercial Cow's Milk. Journal of Agricultural and Food Chemistry 67(17), 4897-4914.

Hufnagl, B., Stibi, M., Martirosyan, H., Wilczek, U., Moller, J.N., Loder, M.G.J., Laforsch, C. and Lohninger, H. 2022. Computer-Assisted Analysis of Microplastics in Environmental Samples Based on muFTIR Imaging in Combination with Machine Learning. Environ Sci Technol Lett 9(1), 90-95.

Indexmundi 2024 Orange Juice Production by Country in MT.

Jadhav E. B., Sankhla M. S., Bhat R.A., and Bhagat D.S., Microplastics from food packaging: An overview of human consumption, health threats, and alternative solutions, Environmental Nanotechnology, Monitoring & Management, 16, 2021, 100608,

Jeffries, C., Rauert, C. and Thomas, K.V. 2025. Quantifying Nanoplastics and Microplastics in Food and Beverages Using Pyrolysis-Gas Chromatography–Mass Spectrometry: Challenges and Implications. ACS Food Science & Technology 5(4), 1536-1545.

Juan, B.; Trujillo, A.-J. Acid and Rennet Coagulation Properties of A2 Milk. Foods 2022, 11, 3648. https://doi.org/10.3390/foods11223648

Kadac-Czapska, K., Jutrzenka Trzebiatowska, P., Mazurkiewicz, M., Kowalczyk, P., Knez, E., Behrendt, M., Mahlik, S., Zaleska-Medynska, A. and Grembecka, M. 2024. Isolation and identification of microplastics in infant formulas – A potential health risk for children. Food Chemistry 440, 138246.

Kaseke, T., Lujic, T. and Cirkovic Velickovic, T. 2023. Nano- and Microplastics Migration from Plastic Food Packaging into Dairy Products: Impact on Nutrient Digestion, Absorption, and Metabolism. Foods 12(16).

Kelebek, H., Selli, S., Canbas, A. and Cabaroglu, T. 2009. HPLC determination of organic acids, sugars, phenolic compositions and antioxidant capacity of orange juice and orange wine made from a Turkish cv. Kozan. Microchemical Journal 91(2), 187-192.

Kubicova, M., Puchta, E., Säger, S., Hug, C., Hofmann, S. and Simat, T.J. 2022. Styrene-acrylonitrile-copolymer and acrylonitrile-butadiene-styrene-copolymer: a study on extractable and migratable oligomers. Food Additives & Contaminants: Part A 39(2), 397-414.

Kutralam-Muniasamy, G., Perez-Guevara, F., Elizalde-Martinez, I. and Shruti, V.C. 2020. Branded milks - Are they immune from microplastics contamination? Sci Total Environ 714, 136823.

Li, D., Shi, Y., Yang, L., Xiao, L., Kehoe, D.K., Gun'ko, Y.K., Boland, J.J. and Wang, J.J. 2020. Microplastic release from the degradation of polypropylene feeding bottles during infant formula preparation. Nature Food 1(11), 746-754.

Liang, Y., Cao, X., Mo, A., Jiang, J., Zhang, Y., Gao, W. and He, D. 2023. Micro(nano)plastics in plant-derived food: Source, contamination pathways and human exposure risks. TrAC Trends in Analytical Chemistry 165.

Lock, A.L. and Shingfield, K.J. 2004. Optimising Milk Composition. BSAP Occasional Publication 29, 107-188.

Mekanna, A.N., Issa, A., Bogueva, D. and Bou-Mitri, C. 2024. Consumer perception of plant-based milk alternatives: systematic review. International Journal of Food Science and Technology 59(11), 8796-8805.

Milk-food 2023 Milk consumption in transition.

Mintenig, S.M., Löder, M.G.J., Primpke, S. and Gerdts, G. 2019. Low numbers of microplastics detected in drinking water from ground water sources. Science of The Total Environment 648, 631-635.

Mohamed Nor, N.H., Kooi, M., Diepens, N.J. and Koelmans, A.A. 2021. Lifetime Accumulation of Microplastic in Children and Adults. Environ Sci Technol 55(8), 5084-5096.

Oliveira, M., Almeida, M. and Miguel, I. 2019. A micro(nano)plastic boomerang tale: A never ending story? TrAC Trends in Analytical Chemistry 112, 196-200.

Olmos, D., Martín, E. and González-Benito, J. 2014. New molecular-scale information on polystyrene dynamics in PS and PS–BaTiO 3 composites from FTIR spectroscopy. Physical Chemistry Chemical Physics 16(44), 24339-24349.

Perez-Cacho, P.R. and Rouseff, R. 2008. Processing and Storage Effects on Orange Juice Aroma: A Review. Journal of Agricultural and Food Chemistry 56(21), 9785-9796.

Pfeiffer, F. and Fischer, E.K. 2020. Various Digestion Protocols Within Microplastic Sample Processing—Evaluating the Resistance of Different Synthetic Polymers and the Efficiency of Biogenic Organic Matter Destruction. Frontiers in Environmental Science Volume 8 - 2020.

PlasticsEurope, E. 2022. Plastics—the facts 2022. . PlasticsEurope https://plasticseurope.org/knowledge-hub/plastics-the-facts-2022/.

Ramsing, R., Santo, R., Kim, B.F., Altema-Johnson, D., Wooden, A., Chang, K.B., Semba, R.D. and Love, D.C. 2023. Dairy and Plant-Based Milks: Implications for Nutrition and Planetary Health. Current Environmental Health Reports 10(3), 291-302.

Rauh, V. and Xiao, Y. 2022. The shelf life of heat-treated dairy products. International Dairy Journal 125.

Rizzi, F.; Juan, B.; Espadaler-Mazo, J.; Capellas, M.; Huedo, P. Lactiplantibacillus plantarum KABP051: Stability in Fruit Juices and Production of Bioactive Compounds During Their Fermentation. Foods 2024, 13, 3851. https://doi.org/10.3390/foods13233851

Rynek, R., Tekman, M.B., Rummel, C., Bergmann, M., Wagner, S., Jahnke, A. and Reemtsma, T. 2024. Hotspots of Floating Plastic Particles across the North Pacific Ocean. Environ Sci Technol 58(9), 4302-4313.

Ščetar, M., Galić, K., Božanić, R., Lisak Jakopović, K., Kurek, M. and Barukčić, I. 2019. Packaging perspective of milk and dairy products. Mljekarstvo 69(1), 3-20.

Shruti, V.C. and Kutralam-Muniasamy, G. 2024. Migration testing of microplastics in plastic food-contact materials: Release, characterization, pollution level, and influencing factors. TrAC Trends in Analytical Chemistry 170.

Smith, B. 2021. The infrared spectra of polymers III: Hydrocarbon polymers.

Ter Halle, A. and Ghiglione, J.F. 2021. Nanoplastics: A Complex, Polluting Terra Incognita. Environ Sci Technol 55(21), 14466-14469.

Visentin, E., Niero, G., Benetti, F. et al. Assessing microplastic contamination in milk and dairy products. npj Sci Food 9, 135 (2025). https://doi.org/10.1038/s41538-025-00506-8

Vethaak, A.D. and Legler, J. 2021. Microplastics and human health. Science 371(6530), 672-674.

Winiarska E., Jutel M., and Zemelka-Wiacek M., The potential impact of nano- and microplastics on human health: Understanding human health risks., Environmental Research, 251, 2, 2024, 118535,

Zhang, Q., Liu, L., Jiang, Y., Zhang, Y., Fan, Y., Rao, W. and Qian, X. 2023. Microplastics in infant milk powder. Environ Pollut 323, 121225.

Zhang, Q., Xu, E.G., Li, J., Chen, Q., Ma, L., Zeng, E.Y. and Shi, H. 2020. A Review of Microplastics in Table Salt, Drinking Water, and Air: Direct Human Exposure. Environ Sci Technol 54(7), 3740-3751.

Zhang, X., Chen, X., Xu, Y., Yang, J., Du, L., Li, K. and Zhou, Y. 2021. Milk consumption and multiple health outcomes: umbrella review of systematic reviews and meta-analyses in humans. Nutr Metab (Lond) 18(1), 7.

Funding information

This study is funded by the EU Horizon 2020 project PLASTICHEAL (GA: 965196).

Declaration of interests

☒ The authors declare that they have no known competing financial interests or personal relationships that could have appeared to influence the work reported in this paper.

☐ The authors declare the following financial interests/personal relationships which may be considered as potential competing interests:

Graphical abstract